



Anammox and denitrification separately dominate microbial N-loss in water saturated and unsaturated soils horizons of riparian zones

Shanyun Wang^a, Weidong Wang^a, Siyan Zhao^a, Xiaomin Wang^a, Mariet M. Hefting^b, Lorenz Schwark^c, Guibing Zhu^{a,*}

^a Research Center for Eco-Environmental Sciences, Chinese Academy of Sciences, Beijing, China

^b Ecology and Biodiversity Group, Department of Biology, Utrecht University, Utrecht, the Netherlands

^c Institute for Geosciences, University of Kiel, Kiel, Germany

ARTICLE INFO

Article history:

Received 28 November 2018

Received in revised form

9 June 2019

Accepted 19 June 2019

Available online 20 June 2019

Keywords:

Anammox

Microbial N-Loss

Riparian zone

Water-saturated soil horizon

N₂O emission

ABSTRACT

Fertilized agroecosystems may show considerable leaching of the mobile nitrogen (N) compound NO₃⁻, which pollutes groundwater and causes eutrophication of downstream waterbodies. Riparian buffer zones, positioned between terrestrial and aquatic environments, effectively remove NO₃⁻ and serve as a hotspot for N₂O emissions. However, microbial processes governing NO₃⁻ reduction in riparian zones still remain largely unclear. This study explored the underlying mechanisms of various N-loss processes in riparian soil horizons using isotopic tracing techniques, molecular assays, and high-throughput sequencing. Both anaerobic ammonium oxidation (anammox) and denitrification activity were maximized in the riparian fringe rather than in the central zones. Denitrifying anaerobic methane oxidation (damo) process was not detected. Interestingly, both contrasting microbial habitats were separated by a groundwater table, which forms an important biogeochemical interface. Denitrification dominated cumulative N-losses in the upper unsaturated soil, while anammox dominated the lower oxic saturated soil horizons. Archaeal and bacterial ammonium oxidation that couple dissimilatory nitrate reduction to ammonium (DNRA) with a high cell-specific rate promoted anammox even further in oxic subsurface horizons. High-throughput sequencing and network analysis showed that the anammox rate positively correlated with *Candidatus* 'Kuenenia' (4%), rather than with the dominant *Candidatus* 'Brocadia'. The contribution to N-loss via anammox increased significantly with the water level, which was accompanied by a significant reduction of N₂O emission (~39.3 ± 10.6%) since N-loss by anammox does not cause N₂O emissions. Hence, water table management in riparian ecotones can be optimized to reduce NO₃⁻ pollution by shifting from denitrification to the environmentally friendly anammox pathway to mitigate greenhouse gas emissions.

© 2019 Elsevier Ltd. All rights reserved.

1. Introduction

Nutrient loading of terrestrial, freshwater, and coastal ecosystems has been occurring on a global scale, which is mainly driven by agricultural activities (Verhoeven et al., 2006). Technological purification has been shown to be the best choice for the reduction of nutrient fluxes into the environment. However, nutrient loading as a result of intensive agricultural practices is typically diffuse or

originates from 'non-point' sources, which makes it hard to address the issue technologically. Riparian zones form the interface areas between freshwater and terrestrial ecosystems and have been shown to efficiently prevent pollutant movement from upland areas into streams (Wang et al., 2002; Hefting et al., 2006). Specifically, riparian zones serve as "sinks" for nitrate (NO₃⁻), which is the most common groundwater pollutant and a precursor to nitrous oxide (N₂O) (Groffman et al., 2002; Hefting et al., 2004). Microbe-driven N reduction processes are key for the creation of NO₃⁻ sinks in riparian zones. It was previously assumed that microbial heterotrophic denitrification was the main NO₃⁻ removal pathway for nitrogen gas (N₂) to the atmosphere (Burgin and Hamilton, 2007). However, the discovery of both anaerobic ammonium oxidation (anammox) and denitrifying anaerobic methane oxidation (damo) greatly changed

* Corresponding author. Research Center for Eco-Environmental Sciences, Chinese Academy of Sciences, China. Address: Box 2871#, Shuangqing Road, Haidian District, 100085, Beijing, China.

E-mail address: gbzhu@rcees.ac.cn (G. Zhu).

this assumption over the past 20 years.

N cycle studies have been conducted for the last 100 years; however, knowledge about the complexity of the underlying process remains limited. This is particularly true for riparian zones due to their high heterogeneity. Denitrification has been one of the most studied processes for the reduction of NO_3^- to N_2 . Traditionally, denitrification has been assumed to only take place under anoxic and anaerobic conditions; however, recently reported evidence indicated that denitrification also happens under oxic conditions (Gao et al., 2010; Marchant et al., 2017). Specifically, anammox could be an alternative N-loss pathway to denitrification, which is performed by autotrophic anammox bacteria that directly oxidize NH_4^+ with NO_2^- to N_2 without emissions of the greenhouse gas nitrous oxide (N_2O). Over the past 20 years, anammox was widely reported in marine (Devol, 2015), freshwater (Zhu et al., 2015), estuary (Naeher et al., 2015), groundwater (Smith et al., 2015; Wang et al., 2017), paddy field (Nie et al., 2015; Shan et al., 2016), and man-made ecosystems (Wang et al., 2015). These studies have identified anammox as a significant contributor to N loss. Moreover, in a number of aerobic environments of artificial ecosystems, aerobic/anoxic/anaerobic micro-environments can form, thus allowing anammox to increase (Third et al., 2001; Vázquez-pađín et al., 2011; Figueroa et al., 2012; Wang et al., 2015). The complexities of the N-cycle were further studied, which led to the discovery of the damo process, where methane (CH_4) is used as electron donor to reduce NO_2^- or NO_3^- anaerobically, mediated by the bacteria *Methyloirabilis* and/or the archaea *Methanoperedens* (Raghoebarsing et al., 2006; Ettwig et al., 2010; Haroon et al., 2013). The damo process links the biogeochemical C and N cycles in a novel way, and has been shown to operate in both inland water and wetland ecosystems (Deutzmann and Schink, 2011; Deutzmann et al., 2014; Hu et al., 2014). These reports significantly promoted the understanding of the global N-cycle. Dissimilatory NO_3^- reduction to ammonium (DNRA), which is a further NO_3^- reduction process, also uses NO_3^- and NO_2^- as substrates under anoxic/anaerobic conditions. In contrast to denitrification, anammox, and damo, DNRA reduces NO_3^- to NH_4^+ instead of N_2 . DNRA is typically considered to be only significant in peripheral environments. Analogous to DNRA, several studies also reported high activity of aerobic DNRA bacteria even if O_2 saturation exceeded 80% (Shan et al., 2016; Roberts et al., 2014). In these microbe-mediated NO_3^- reduction processes, NH_4^+ is generated by DNRA as an end product, which is then used as a substrate for anammox. Subsequently, NH_4^+ is oxidized to NO_3^- by ammonia-oxidizing archaea (AOA) & bacteria (AOB), and nitrite-oxidizing bacteria (NOB), thus allowing the recycling of substrates necessary for these microbial processes. The symbiotic and competitive mechanisms among denitrification, anammox, damo, and DNRA demonstrate the complexity of the N cycle, especially in riparian zones. Overall, the discovery of novel microbe-mediated N transfer mechanisms, with new taxa and functions, challenge existing knowledge about the N cycle and spatiotemporal variations in riparian zones. This limited understanding warrants further research to better understand the underlying biogeochemical processes.

In riparian soil profiles, the zone around the groundwater table has been identified as an important hotspot for biogeochemical cycles (Naiman and Décamps, 1997; McClain et al., 2003; Hancock et al., 2005; Naeher et al., 2015). Fluctuations of the groundwater table control water saturation and redox conditions in wetland soils, which then drive N-cycling and the involved differences in microbial rates (Hefting et al., 2004). In general, saturated soils below the groundwater table contain lower oxygen concentrations compared to upper unsaturated soils. In a number of riparian zones along lakes, however, surface water can infiltrate the underlying soil. This results in the oxygenation of the saturated soil with

groundwater, which leads to high oxygen content and long retention times. Since the organic matter content is lower in deeper soil horizons, N-loss is predominantly driven by more dominant autotrophic microbial processes (Zhu et al., 2018a). In contrast, in soil horizons above the groundwater table, N-loss is dominated by heterotrophic processes due to an increase of organic matter from the litter layer, root exudates, and microbial residues (Wang et al., 2012a, b; Hefting et al., 2004, 2006). Based on previous studies on microbial N-cycles in wetland ecosystems (Hefting et al., 2004; Wang et al., 2012a, b; Zhou et al., 2015; Zhu et al., 2011, 2013a, b), this study proposes that heterotrophic denitrification, autotrophic anammox, and damo have different degrees of contribution to N-loss of riparian zone profiles above and below the groundwater table. Moreover, increased anammox with N-loss is accompanied by decreased N_2O emissions, since N-loss via anammox does not lead to N_2O emission.

Given this background, the objectives of present study are: (i) to explore the distribution and biogeochemistry of denitrification, anammox, DNRA, and damo processes in water-saturated and water-unsaturated riparian soil horizons. Furthermore, to quantify the contribution of each microbial process to the overall N-loss, NO_3^- -removal, and mitigation of N_2O emission; (ii) to investigate the underlying mechanisms and to provide a complete overview of the Nitrite-producing or -removing processes related to anammox using isotopic tracing, (q)PCR, clone, high-throughput sequencing, and molecular ecological network analyses.

2. Materials and methods

2.1. Study site

Lake Baiyangdian is the largest natural freshwater lake group of North China with well-developed riparian zones that are an anammox hotspot (Zhu et al., 2013a, b). Increasing sewage and wastewater influx from an upstream city and agricultural runoff led to the eutrophication of the lake. The lake Baiyangdian group consists of approximately 140 lakes, with a total area of 366 km^2 at a water level of 10.5 m above the sea level and a water depth of 2 m on average. The 9400 ha of reed-bed/ditch landscape has more than 3700 ditches (approximately 24.8 km^2), dominated by *Phragmites australis* with root channels densely populating the 0–1.0 m level below the surface of the reed bed. The water level of Lake Baiyangdian rose from a depth of 50–60 cm in 2015 to 20–30 cm in 2017. These fluctuations of the water level allowed detailed investigations of the N cycle mechanisms, particularly those related to N-loss such as anammox, denitrification, and damo on both spatial and temporal scales in the riparian zone.

The study site was a reed bed with 24 m width and 26 m length (38°54′49″ N, 115°57′56″ E) in Lake Baiyangdian, with ditches along the riparian zones at 0.6–2.5 m depth and 10–15 m width. The water at this site fluctuated vertically between 0.6 and 1.4 m. Samples were collected from 1 m, 3 m, and 6 m from the water in the fringe riparian zone, and from 12 m from the water in the central riparian zone (Fig. 1; Fig. S1). At each sampling site, three soil cores (5 cm diameter and 100 cm depth; Column cylinder soil sampler, New Landmark, Beijing) were collected from plots (1.2 m × 1.2 m) using Plexiglas core tubes. Samples were hermetically sealed and transported to the laboratory on ice. Sampling was conducted in September 2015 and 2017 before and after the increase of the groundwater level. In the laboratory, cores were immediately sliced at 20-cm intervals and mixed at every depth layer in each site to form one composite sample. For each mixed soil sample, one subsample was incubated to determine microbial activity. A further subsample was sieved through a 2.0-mm filter for chemical analyses. Subsamples were stored at -80°C for subsequent molecular analysis. At the same

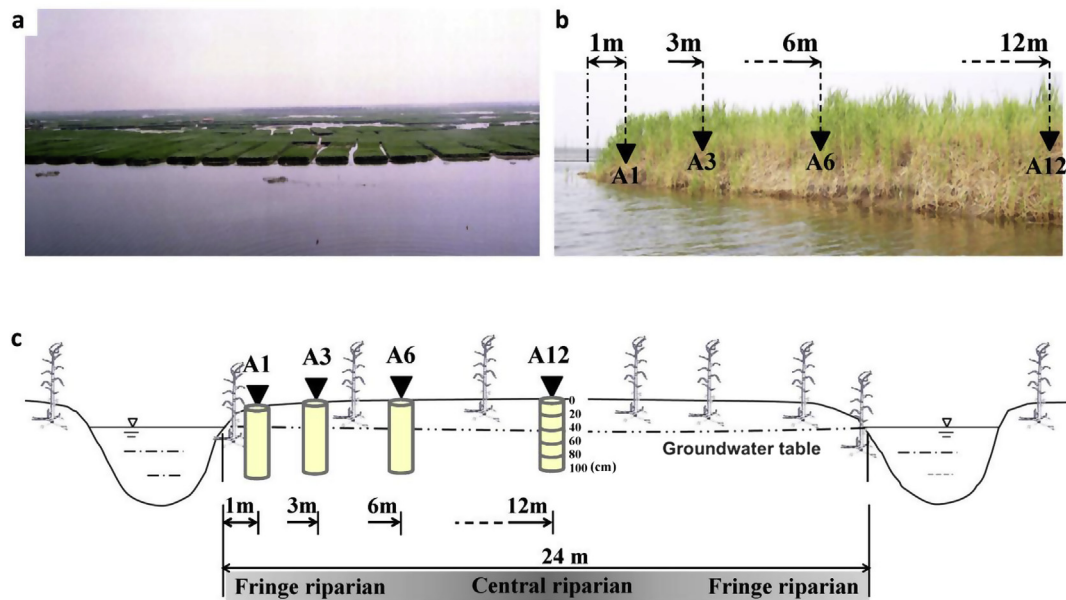


Fig. 1. The sampling soil profile in a riparian zone. (a) A view of the reed-bed/ditch landscape in Baiyangdian Lake; (b) the view of the sampling riparian zone; (c) sampling site details. Soil profiles (A1, A3, A6 and A12) represent the sampling site 1 m, 3 m, 6 m and 12 m from the water in the fringe and central riparian zone, respectively. The soil cores were 100 cm depth and 20-cm intervals with the groundwater table of approximately 40 cm depth.

sampling site, water level and N_2O emission flux were also measured twice per month in September, October, and December 2015 and 2017 before and after the increase of the groundwater level.

2.2. DNA extraction, (q)PCR assay, and clone sequencing

Genomic DNA was extracted from 0.33 g freeze-dried soil using a FastDNA SPIN Kit for Soil (MP Biomedicals, Solon, OH, USA). Purity and quantity of the extracted DNA were determined by a NanoDrop spectrophotometer (ND-1000; Thermo Fisher Scientific, Wilmington, Delaware USA). Quantitative PCR (qPCR) assays were conducted using fluorescent dye II SYBR-Green in an ABI 7500 Fast Real-Time PCR system (Applied Biosystems, Foster City, CA, USA). Functional or 16S rRNA genes of nitrite-removing bacteria were quantified, i.e., the hydrazine synthase β -subunit (*hzsB*) gene of anammox bacteria, the *cd1* or copper nitrite reductase (*nirS* or *nirK*) gene of denitrifiers, the cytochrome *c* nitrite reductase (*nrfA*) gene of DNRA bacteria, and the particulate methane monooxygenase (*pmoA*) and putative NO dismutases (*Nod*) genes of damo. The primer pairs were HSBeta396F/HSBeta742R for *hzsB* (Wang et al., 2012a, b), cd3aF/R3cd for *nirS* (Michotey et al., 2000; Throback et al., 2004), FlaCu/R3Cu for *nirK* (Hallin et al., 1999; Di et al., 2014), *nrfAF2aw-nrfAR1* for *nrfA* (Mohan et al., 2004; Welsh et al., 2014; Song et al., 2014), and p1F/p1R, p2F/p2R and nod1446F/nod1706Rv2 for *pmoA* 16S rRNA and the functional gene *Nod* (Ettwig et al., 2009; Zhu et al., 2018a, b, c), respectively. Genes involved in ammonia oxidation were also quantified using the primers *amoAF/amoAR* for the bacterial ammonia monooxygenase α -subunit (*amoA*) gene (Wang et al., 2011) and *arch-amoAF/arch-amoAR* for archaeal *amoA* (Francis et al., 2005; Wang et al., 2011). Each standard curve was generated with 10-fold serial dilutions of plasmid DNA, containing the respective genes. The known concentration of plasmid DNA was obtained from our laboratory, and the isolated details of plasmid DNAs have been described by Wang et al. (2018). Melting curves were generated after each assay to verify the specificity of amplification. All amplification efficiencies ranged of 90–110% and all correlation coefficients (R^2) exceeded 0.98. All tests were performed in triplicate.

PCRs were conducted to amplify AOA *amoA*, AOB *amoA*, and DNRA *nrfA* genes on a C1000 Thermal Cycler (Bio-Rad, Hercules, USA). Purified amplicons were ligated to pGEM-T Easy (Promega, Madison, WI, USA), and then transformed to *Escherichia coli* JM109 competent cells (Promega, Madison, WI, USA) following the manufacturer's instructions. 96 clones were picked randomly for each of the amplicons, and screened for the presence of targeted gene fragments using T7 and SP6 vector primers for PCR assays. Positive amplicons were then screened with restriction endonucleases *Hha* I and *Hae* III (TAKARA, Dalian, China). 2–3 representative clones from each digestion pattern were sequenced with an ABI PRISM 3730XL sequencer (Applied Biosystems, Foster City, CA, USA). Sequences with identities of at least 97% were clustered into the same operational taxonomic units (OTUs) using DOTUR software version 1.53 (Schloss and Handelsman, 2005). The obtained sequences were deposited in GenBank under accession numbers KY062573–KY062589 (AOA), KY062590–KY062613 (AOB), and MF575852–MF575901 (DNRA). Phylogenetic trees were constructed by the neighbor-joining (NJ) method in the MEGA package, version 5.0 (Tamura et al., 2007). More details on the primers and thermal profiles are listed in Table S1.

2.3. High-throughput sequencing and network analysis

Approximately 1 μg of genomic DNA was used to prepare high-throughput sequencing libraries for targeting the anammox *hzsB* gene with the barcoded primer pairs HSBeta449F and HSBeta742R using the DNA Library Prep kits (NEB Next, Ultra, CA, USA) (Zhao et al., 2018; Wang et al., 2018). Purified amplicons were sequenced on the Illumina HiSeq 2500 platform (Illumina, San Diego, CA, USA) using the PE250 sequencing strategy. The nucleic acid sequences were quality filtered to an equal length (~292 bp), corrected frame-shifts, no ambiguous bases (N), and barcode or primer mismatches, using QIIME (Caporaso et al., 2010) and Mothur (Schloss et al., 2009). OTUs were clustered at 97% similarity using Mothur (Schloss et al., 2009). Heatmaps were constructed using Heml (Deng et al., 2014) indicating the relative abundances of anammox species. Correlation-based network analysis was conducted to explore the potential co-

occurrence mechanism of anammox taxa at the OTU level according to Zhou et al. (2010). The utilized pipeline was provided by the Institute of Environmental Genomics, University of Oklahoma. All sequence reads were deposited into GenBank under the accession number PRJNA523106.

2.4. Measurements of microbial N-cycle processing rate using the ^{15}N -tracer technique

Homogenized soil samples (~3.3 g each) from each of the 20 cm-interval depth layers were separately transferred to 12-mL glass vials (Exetainer, Labco, UK), filled with sterile water. These were incubated at the same temperature as measured at the test site in a water bath. The DO concentration of the resulting slurry was slightly adjusted by flushing He (99.9%) and O_2 (99.9%) until they became similar to *in situ* conditions ($\pm 5\%$ standard deviation).

The residual N-compounds of the resulting slurries were input to correct the initial ratios of $^{14}\text{N}/^{15}\text{N}$ (r_{14}) in related incubation vials (Risgaard-Petersen et al., 2004; Trimmer et al., 2006; Wang et al., 2018). The rates of N-cycling processes were determined by adding ^{15}N -amended ammonium and NO_3^- ($\text{Na}^{15}\text{NO}_3$ [99.19% ^{15}N], $(^{15}\text{NH}_4)_2\text{SO}_4$ [99.16%], and $\text{Na}^{15}\text{NO}_2$ [98.17%]). Final concentrations ranged from 5% to 10% of the initial background concentration, which minimized over- or under-estimation of the potential rate. The natural abundance of ^{15}N in the soil was very low, especially compared to the ^{15}N -amended additional substrates; therefore, all initial N-compounds were assumed to be ^{14}N based on isotopic calculation (Nielsen, 1992; Trimmer et al., 2006; Wang et al., 2018). Three parallel assays were conducted for each sample and each treatment, following previously described protocols with modifications (Granger and Sigman, 2009; Füssel et al., 2012; Wang et al., 2018; Zhu et al., 2018a, b, c).

To determine anammox and denitrification rates, ^{15}N stock solution was injected into each of the incubation treatments, (1) $^{15}\text{NH}_4^+$ (5.9–20.3 μM , final concentration) + $^{14}\text{NO}_3^-$, (2) $^{15}\text{NO}_3^-$ (4.2–30.4 μM) (Risgaard-Petersen et al., 2004; Trimmer et al., 2006; Wang et al., 2018). 200 μL of ZnCl_2 solution (7 M) was added to terminate the incubation at each time point (0 h, 2 h, 4 h, 6 h, 8 h, and 12 h). For slurries amended with $^{15}\text{NH}_4^+$ and $^{14}\text{NO}_3^-$, $^{29}\text{N}_2$ had accumulated due to anammox production. This was used to calculate the anammox process in every soil layer. However, slurries amended solely with $^{15}\text{NO}_3^-$ produced all of the ^{15}N -amended N_2 , $^{29}\text{N}_2$, $^{29}\text{N}_2$, and $^{30}\text{N}_2$, while denitrification was the only source of $^{30}\text{N}_2$. Both treatments were used to calculate the relevant denitrification processes.

The ammonium oxidation rate was measured as the production rate of $^{15}\text{NO}_2^-$ from $^{15}\text{NH}_4^+$ under oxic conditions. A known quantity of the $^{15}\text{NH}_4^+$ stock solution was injected to 5.9–8.7 μM , and the ratios of $^{14}\text{NH}_4^+ : ^{15}\text{NH}_4^+$ were calculated. Incubations were terminated at each time point (0 h, 2 h, 4 h, 6 h, 8 h, and 12 h). To assess the $^{15}\text{NO}_2^-$ yield, 16.5 mM (final concentration) of sulfamic acid was added to completely reduce $^{15}\text{NO}_2^-$ to $^{29}\text{N}_2$ (Granger and Sigman, 2009; Füssel et al., 2012; Wang et al., 2018; Zhu et al., 2018a, b, c) for conversion exceeding 12 h, to minimize underestimation of the rate. The produced $^{29}\text{N}_2$ was then used to calculate for the ammonium oxidation rates using the corrected ratio of $^{14}\text{NH}_4^+ : ^{15}\text{NH}_4^+$.

For the DNRA rate, 100 μL of diluted $^{15}\text{NO}_2^-$ stock solution was injected to 0.1–0.4 μM (final concentration), while the $^{14}\text{NO}_2^- : ^{15}\text{NO}_2^-$ ratio was calculated for the final rate correlation. At each time point (0 h, 2 h, 4 h, 6 h, 8 h, and 12 h), the reaction was stopped by adding hypobromite with a final concentration equaling that of $^{15}\text{NO}_2^-$, followed by 12 h of incubation to completely convert the produced $^{15}\text{NH}_4^+$ to $^{30}\text{N}_2$ (Lam et al., 2009; Füssel et al., 2012; Wang et al., 2018; Zhu et al., 2018a, b, c). The produced $^{30}\text{N}_2$ was then used to calculate the DNRA rates with the corrected ratio of $^{14}\text{NO}_2^- : ^{15}\text{NO}_2^-$.

The NO_3^- reduction rate was measured by adding 100 μL of diluted $^{15}\text{NO}_3^-$ stock solution to a final 4.2–6.7 μM , and then, 100 μL of saturated mercuric chloride were injected to terminate the reaction at each time point (0 h, 2 h, 4 h, 6 h, 8 h, and 12 h). Then, 16.5 mM (final concentration) of sulfamic acid was added and incubated for more than 12 h to completely reduce $^{15}\text{NO}_2^-$ to $^{29}\text{N}_2$ (Granger and Sigman, 2009; Füssel et al., 2012; Wang et al., 2018; Zhu et al., 2018a, b, c). This was then used to calculate the NO_3^- reduction rates using the actual ratio of $^{14}\text{NO}_3^- : ^{15}\text{NO}_3^-$.

Atmospheric air was used to generate both standard curve and reference air, which were measured together with the incubations of soil samples (Risgaard-Petersen et al., 2004; Wang et al., 2018; Zhu et al., 2018a, b, c). Several glass vials (12 mL volume; Exetainer, Labco, UK) were filled with demineralized water without headspace and equilibrated with atmospheric air at *in situ* temperature. Subsequently, 8 mL of the water was removed and replaced with high-purity He (99.9%). Then, 0, 30, 60, 90, and 120 μL of air were injected into the standard curve vials, respectively. All glass vials were shaken for at least 1 min to achieve equilibrium between water and headspace. Standard curves were used to linear regress the total signal versus the yield of each $^{15}\text{N}-\text{N}_2$. Then, the concentrations of the produced $^{15}\text{N}-\text{N}_2$ in samples were calculated. A linear regression was generated between the labelled $^{15}\text{N}-\text{N}_2$ concentration shift over time, with coefficients (R^2) of >0.60 and a significance level of $p < 0.05$. The $^{15}\text{N}-\text{N}_2$ concentrations were measured by IRMS (MAT253 with Gasbench II, Thermo Electron Corporation, USA; Table S2) with a minimum detectable rate of about 0.001 nmol-N $\text{g}^{-1} \text{h}^{-1}$ at the Institute of Tibetan Plateau Research, Chinese Academy of Sciences.

2.5. Measurement of the damo rate using the ^{13}C -tracer technique

The potential damo rates in the riparian zone were determined based on $^{13}\text{C}-\text{CO}_2$ production using the $^{13}\text{C}-\text{CH}_4$ stable isotope technique described in Shen et al. (2015) and Zhu et al. (2018a, b, c). Soil slurries for each sample were pre-incubated in triplicate under anoxic conditions to completely deplete residual NO_3^- and O_2 . Rates were calculated via linear regression of the CO_2 yield and incubation time. The linear correlation exceeded 0.90, and the ratio of $^{13}\text{C}-\text{CO}_2$ to total CO_2 in the negative controls remained consistent with that of atmospheric air. The measurements were performed using IRMS (Delta V Advantage, Thermo Electron Corporation, USA) with a minimum detectable rate of approximately 0.002 nmol-C $\text{g}^{-1} \text{h}^{-1}$ at the Research Center for Eco-Environmental Sciences, Chinese Academy of Sciences.

2.6. Analytical procedures for soil environmental variables

NH_4^+ , NO_2^- , and NO_3^- in the soil were extracted using 2 mol L^{-1} KCl and were analyzed by a continuous flow analyzer (Seal Analytical, UK). The soil pH was analyzed in a 1:5 soil:water (w/v) suspension by a DELTA 320 pH Analyzer (Mettler Toledo, USA) (Bao, 2000). The total organic matter (TOM) was determined by oxidizing potassium dichromate and sulphuric acid (Bao, 2000). The total nitrogen (TN), total carbon (TC), and total sulfur (TS) were measured by an elemental analyzer system (Vario EL III Analyzer, Germany). After soil cores were dug, the DO and temperature were immediately analyzed by an optical DO sensor (4.5 cm diameter) equipped with a YSI Model 600 XLMV2 multi-probe sonde. The sensor was slowly lowered to the soil sample to prevent mixing. Measurements were processed in triplicate for quality assurance/quality control.

2.7. Measuring N_2O concentrations and fluxes

The N_2O emission flux was measured using the closed-chamber technique with triplicate chambers for each sampling test (Wang et al., 2006). The stainless-steel chambers consisted of a pedestal and an upper chamber. The bottom rim of the pedestal was pushed into the soil and the top rim was filled with water, thus creating an airtight seal. The upper chamber was equipped with brushless fans, driven by two batteries to mix the chamber headspace. A temperature probe reported the real-time air temperature of the chamber headspace. N_2O concentrations were immediately detected after sampling, using a gas chromatography (GC- μ ECD, Agilent 4890D, USA) with a precision of $\pm 2.8\%$. One reference gas was measured per six samples. N_2O flux was calculated using the linear regression of the concentration of the N_2O in the chamber headspace to a function of time at the air temperature of the chamber headspace. The R^2 values derived from the linear regression exceeded 0.90.

2.8. Statistical analysis

The cell-specific rate was calculated by dividing microbial activity by the abundance of corresponding functional genes, assuming that i) all cells were active and had equal activity levels, and that ii) all cells had a unique targeting functional gene copy, except for AOB with an average 2.5 copies per cell (Jia et al., 2009). The resulting data were presented as mean value \pm standard deviation (s.d.). Pearson's correlation analysis, analysis of variance (ANOVA), and t -test analyses were computed using SPSS software 22.0 for Windows (SPSS Inc, USA). The coefficient of variation (CV) was used to evaluate the variations of anammox bacterial abundance. Redundancy analysis (RDA) was used to investigate the relationship among the rate and abundance of anammox bacteria and the environmental factors. The results were plotted in CANOCO 4.5 (Ithaca, NY, USA). All data in this study below the detection limit were processed as zero and the level of statistical significance was $\alpha = 0.05$ ($p \leq 0.05$).

3. Results

3.1. Physicochemical characteristic of the sampled soil profile

In general, NH_4^+ and NO_3^- concentrations were not significantly different between the fringe riparian zone (A1, A3, and A6) and the central riparian zone (A12) (Fig. 2). Higher NH_4^+ and NO_3^- concentrations were detected at A3. NO_2^- showed an increasing trend from

waterward to landward, peaking in the central riparian zone. Due to the infiltration of lake water, containing high oxygen levels ($>5 \text{ mg L}^{-1}$), the DO saturation in subsurface groundwater decreased from the fringe riparian zone ($28.06 \pm 5.86\%$ at A1) to the central riparian zone ($20.57 \pm 6.17\%$ at A12).

In contrast, the vertical distribution from the surface to the subsurface showed that NH_4^+ , NO_2^- , NO_3^- , and TN concentrations were higher in the surface soils (0–20 cm), and rapidly decreased with depth (ANOVA, $p < 0.05$; Fig. 2). The DO saturation in subsurface groundwater also showed a decreasing trend. The TOM level in the saturated layer soil ($4.89 \pm 1.00\%$) was lower than in the surface soils above the water level ($5.54 \pm 1.08\%$).

3.2. Abundance and activity of anammox, damo, and denitrifiers

The anammox bacteria-specific hydrazine synthase (*hzsB*) gene was investigated in the top 100 cm of soil from the riparian zone. All samples above the groundwater level (40 \pm 5 cm depth) showed negative results, with a detection limit of approximately 10^3 gene copies g^{-1} dry soil (Fig. 3). Below the groundwater level (40–100 cm depth), qPCR assays showed that the abundance of anammox bacteria ranged from 1.75×10^7 to 6.10×10^7 copies g^{-1} (0.04–0.62% of the total bacterial 16S rRNA gene). In the central riparian zone, the abundance of anammox bacteria varied more significantly throughout the soil profile (coefficient of variance, CV = 35.4%; Fig. 3d). However, the other samples collected from the fringe riparian zone near the lake (A1, A3, and A6; Fig. 3a, b, and c) showed little variation (CV = 6.1–15.3%).

The ^{15}N -tracing technique (Fig. 3) showed that anammox activity was absent above the groundwater table (at 40 cm depth), which is consistent with the results based on molecular techniques. Below the groundwater table, anammox activity was detected, and ranged from 0.010 ± 0.001 to $0.220 \pm 0.001 \text{ nmol N g}^{-1} \text{ h}^{-1}$. Across all vertical profiles, the activity was consistently lowest in the 40–60 cm layer, contributing 5.4–23.5% to N loss. Both anammox activity and its contribution to N loss increased with depth, accounting for up to 63.9%. Furthermore, the anammox activity in the central riparian zone was significantly lower than in the three samples collected from the fringe riparian zone (independent samples t -test, $t = 2.652$, $df = 15.141$, $p = 0.018$). The highest anammox activity (0.098 ± 0.047 to $0.220 \pm 0.001 \text{ nmol N g}^{-1} \text{ h}^{-1}$) was detected at A3, which is consistent with NH_4^+ and NO_3^- distributions. These results further showed that anammox plays an important role in N loss in subsurface saturated soil horizons, especially in deeper layers. In contrast, the contributions of

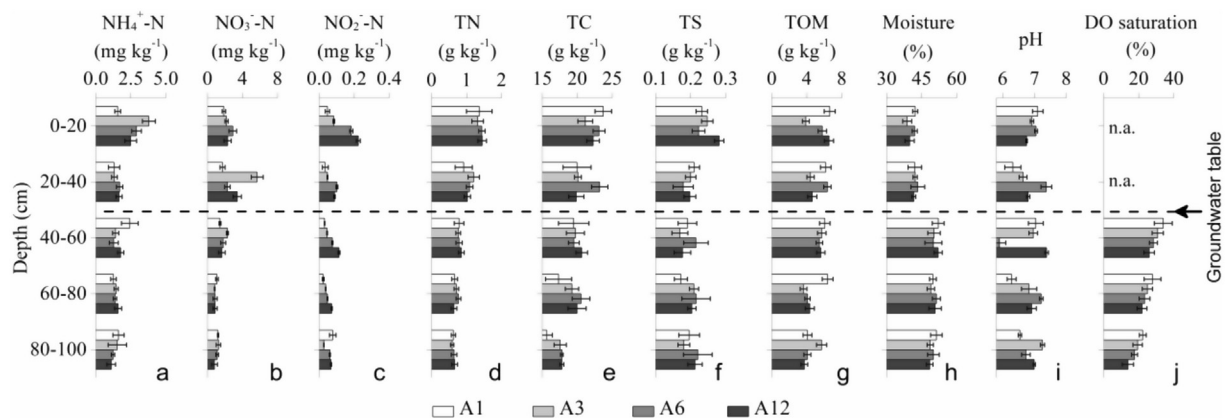


Fig. 2. The physico-chemical characteristics of the sampled soil profiles. Data bars are mean values; error bars represent standard deviations from replicates ($n = 3$). Bar colors represent the sampling site of A1, A3, A6 and A12, respectively. n. a. indicates 'No data'.

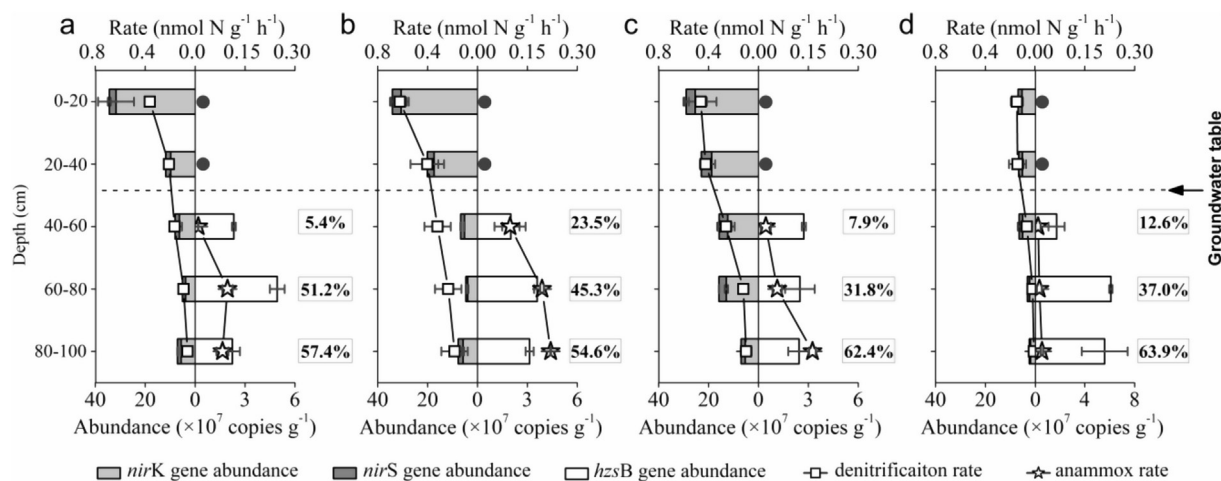


Fig. 3. Biogeographical distribution of the abundance and activity of anammox and denitrifying bacteria in soil profiles of the riparian zone in Baiyangdian Lake, China. a–d represent the sampling site of A1, A3, A6 and A12. A solid circle indicates levels below the detection limit ($<10^3$) with no positive ^{15}N tracing result across replicates ($n = 3$). The percentage in the gray rectangular box indicates the average contribution of N loss via anammox process.

anammox were negligible or even absent above the groundwater table. In addition, Pearson correlation analysis showed that neither anammox abundance nor activity were significantly correlated with any physicochemical parameter. However, the maximal correlation coefficients were all obtained with NO_3^- , abundance vs NO_3^- ($r = -0.611$, $p = 0.108$), and activity vs NO_3^- ($r = -0.635$, $p = 0.091$), and NO_2^- ($r = 0.503$, $p = 0.204$) (Table S5). Thus, NO_3^- may be the key factor for controlling the contribution of anammox to N loss in water saturated soils.

The results of the qPCR assay indicate that both denitrifier *nirS* and *nirK* gene copies peaked in the surface soil and decreased with depth. The *nirS* gene copy ranged from $5.30 \pm 0.15 \times 10^6$ to $4.17 \pm 0.56 \times 10^7$ copies g^{-1} , supplying approximately 0.03–0.40% of the total bacteria. *nirK* ranged from $1.75 \pm 0.65 \times 10^7$ to $6.10 \pm 0.13 \times 10^7$ copies g^{-1} , which was 0.1–1.4% of the total bacterial abundance. In general, *nirK* was consistently higher than *nirS* at all depths in all tested samples. Furthermore, the average abundances of the *nirK* and *nirS* genes were higher in the fringe riparian zone than in the central riparian zone.

Denitrification, measured using the ^{15}N -tracer method (Fig. 3), was detected in every layer of all samples, ranging from 0.012 ± 0.015 to 0.622 ± 0.071 $\text{nmol N g}^{-1} \text{h}^{-1}$. The highest denitrification levels were observed in surface soil samples, which decreased with depth. Denitrification was significantly positively correlated with the abundance of denitrifying genes ($r = 0.855$, $p < 0.001$, $n = 20$). Furthermore, denitrification activity in the central riparian zone was significantly and consistently lower than in the fringe riparian zone (ANOVA, $F = 3.671$, $df = 3$, $p = 0.022$), with the highest level at A3 ($p < 0.001$) (Fig. 3c).

Based on the $^{13}\text{CH}_4$ -tracer approach, no $^{13}\text{CO}_2$ was detected from methane in any of the tested samples, even after 26 days of incubation. This indicates little to no damo activity, which was consistent with the results of molecular analysis, where no damo bacterial 16S rRNA and functional genes were detected.

The specific anammox cellular activity in subsurface saturated soil horizons ranged from 0.005 to 0.168 $\text{fmol N cell}^{-1} \text{d}^{-1}$ (Fig. S2). In contrast, cell-specific denitrifying activity ranged from 0.012 to 0.122 $\text{fmol N cell}^{-1} \text{d}^{-1}$. In the central riparian zone, the cell-specific activity of anammox and denitrification were both lower than in the fringe riparian zone, especially for the cell-specific activity of anammox (independent samples *t*-test, $t = 2.866$, $df = 14.701$, $p = 0.012$). Moreover, the cell-specific denitrifying rate

decreased with depth, in contrast to the cell-specific anammox rate, which also exceeded the denitrification rates. The cell-specific activities indicate that denitrifiers were more active in water-unsaturated soil horizons than in water-saturated soils, whereas anammox bacteria were more active in saturated soil horizons than in unsaturated soils.

3.3. Intraspecific microbial characteristic of anammox bacteria

High-throughput sequencing and molecular ecological network analysis were used to explore the anammox community in the saturated soil layers (60–80 cm and 80–100 cm depths). Here, anammox could play an important role in N-loss. A total of 77 OTUs were clustered from a total 298,362 effective sequences. These OTUs belonged to four major anammox genera, including *Candidatus Brocadia* (*Ca. B. fulgida* (62.2%), *Ca. B. anammoxidans* (34.1%), *Ca. Jettenia* sp. (3.5%), *Ca. Kuenenia* sp. (0.2%), and *Ca. Scalindua* sp. (0.07%) (Fig. 4 a; Fig. S3; Table S6). The dominant *Ca. Brocadia* also formed an important link among anammox taxa both in the fringe and center of the riparian zone, but it contained different species. *Ca. B. fulgida* (OTU 75) was the key species in the riparian center, while *Ca. B. anammoxidans* (OTU 29) was the key species in the fringe zone (Fig. 4 b).

Furthermore, RDA analysis showed that anammox activity was significantly correlated with *Ca. Kuenenia* (Pearson's $r = 0.714$, $p = 0.047$) and *Ca. Scalindua* ($r = 0.810$, $p = 0.015$), and negatively associated with the total anammox abundance ($r = -0.429$, $p = 0.289$) and *Ca. Brocadia* ($r = -0.437$, $p = 0.279$) ($n = 8$; Fig. 4c; Table S5). Thus, anammox activity in the oxic saturated soil horizons was not necessarily driven by total anammox abundance or by dominant groups, but rather by key taxa, such as *Ca. Kuenenia*.

3.4. Interspecific microbial mechanisms of anammox with other N cycle processes

The biogeochemical mechanisms of the N cycle in riparian subsurface saturated soil horizons (80–100 cm deep) were also investigated. Here, anammox dominated the N-loss over denitrification. Nitrite-removing and nitrite-producing activities were measured because nitrite has previously been assumed as the key substrate for anammox bacteria (Fig. 5). For NO_2^- -producing pathways, NH_4^+ oxidation occurred at high rates (3.34 – 8.45 nmol N g^{-1}

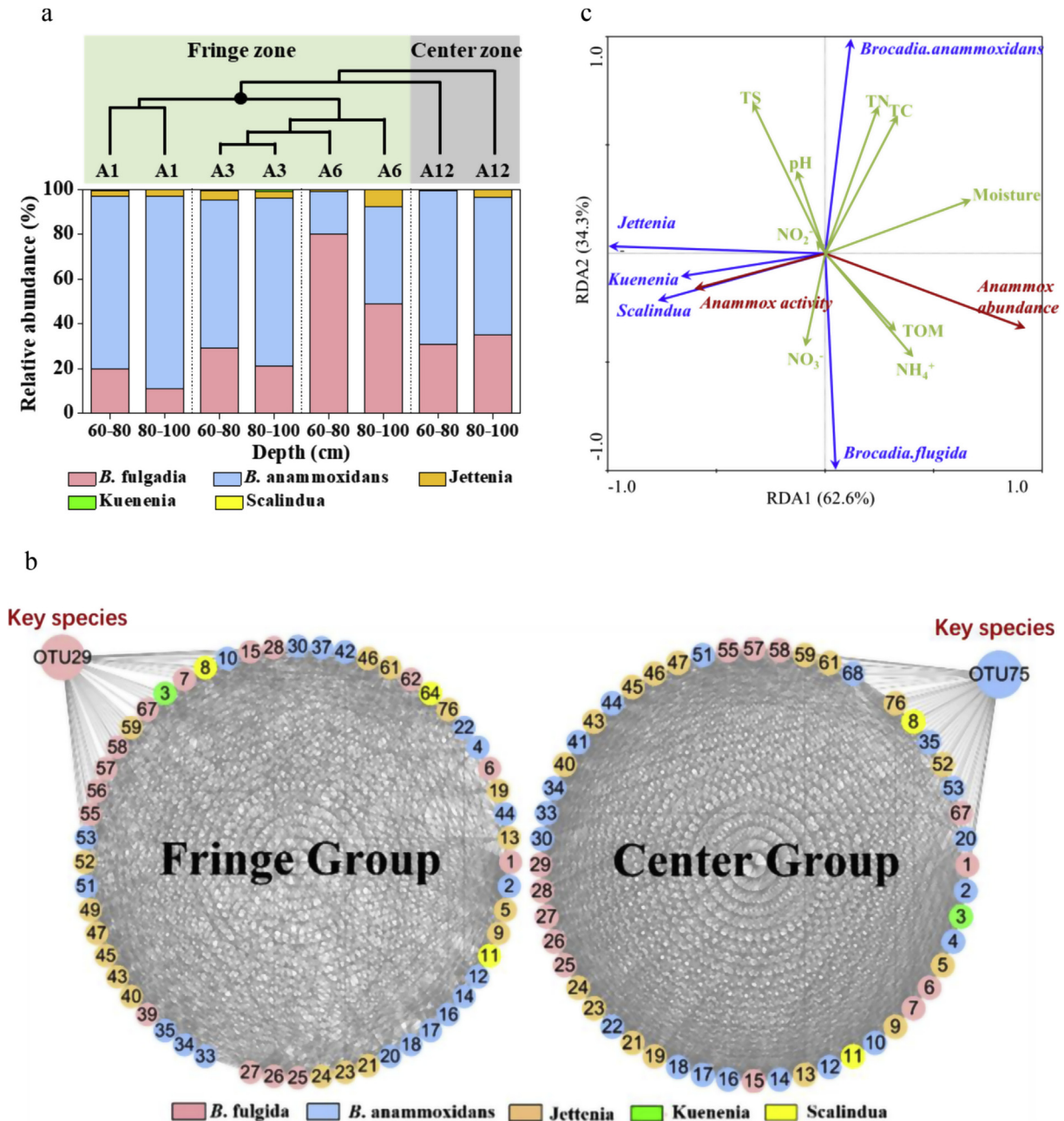


Fig. 4. High-throughput sequencing analysis of the anammox specific *hzsB* functional gene in soil samples from the 60–80 cm and 80–100 cm layers. (a) Bar graphs of the relative abundances of dominant anammox microbes. (b) Molecular ecological networks of the key anammox microbes in Fringe Group and Center Group, respectively. The nodes represent OTUs; the colors of nodes represent different anammox species. The modules, named Fringe Group and Center Group, is the group of OTUs that are highly connected among themselves in Fringe zone and Center zone, respectively. The node links show the interactions between two OTUs within the module. (c) RDA analyses illustrate the relationship among the community composition, rate and abundance of anammox bacteria and the environmental factors. The correlations are represented by the arrow length and angle. (For interpretation of the references to color in this figure legend, the reader is referred to the Web version of this article.)

h^{-1}), which was significantly higher than NO_3^- reduction ($2.05\text{--}2.85 \text{ nmol N g}^{-1} \text{ h}^{-1}$). This indicates that the NO_2^- required for anammox and denitrification was mainly provided by NH_4^+ oxidation ($54.0\text{--}80.4\%$), rather than by NO_3^- reduction. For NO_2^- -removing processes, the NO_2^- oxidation rate was significantly lower than that of the NH_4^+ oxidation rate (paired-sample t -test, $t = 5.737$, $\text{df} = 3$, $p = 0.011$). The other two NO_2^- -removing processes (denitrification and anammox) were both lower compared to the other processes that produce NO_2^- . The total fluxes of NO_2^- production ($6.20\text{--}10.51 \text{ nmol N g}^{-1} \text{ h}^{-1}$) were significantly higher than those of

NO_2^- removal ($2.47\text{--}4.91 \text{ nmol N g}^{-1} \text{ h}^{-1}$) in all samples (paired-sample t -test, $t = 10.090$, $\text{df} = 3$, $p = 0.002$). This suggests that other NO_2^- -removing processes may be occurring in riparian subsurface saturated soil horizons. The DNRA rate ranged from 1.50 to $3.11 \text{ nmol N g}^{-1} \text{ h}^{-1}$. DNRA contributed to approximately 51.0–68.4% of the NO_2^- -removing processes, followed by NO_2^- oxidation (22.7–46.1%), denitrification (0.5–4.0%), and anammox (0.9–4.8%). DNRA and NH_4^+ oxidation activities were also higher in the fringe riparian zone than in the central riparian zone, which is consistent with the anammox activity (Fig. 5). At the same time,

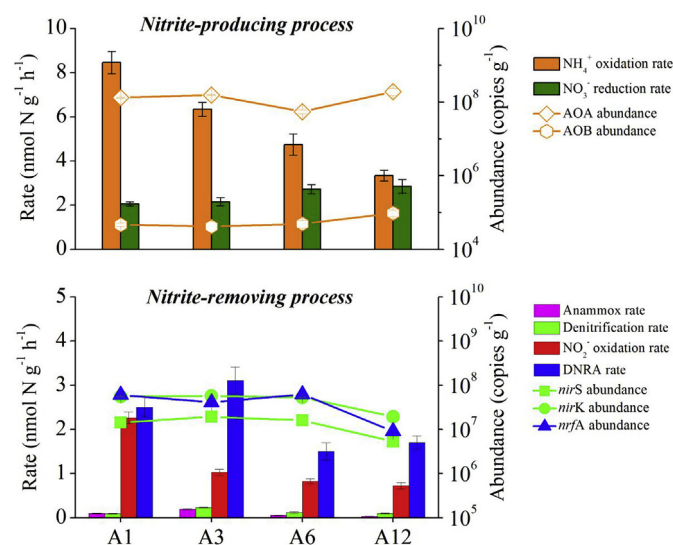


Fig. 5. The activity of microbial nitrite-producing (top) and nitrite-removing (bottom) processes and the relative abundance of the higher-rate nitrite conversion processes in the riparian subsurface saturated soil horizons (80–100 cm). Error bars represent S.D. ($n = 3$).

DNRA was coupled with high NH₄⁺ oxidation activity, which provides a significant proportion of the NH₄⁺ required for anammox.

The abundance of DNRA and NH₄⁺ oxidation related microbes were quantified using qPCR (Fig. 5). Here, cell number (based on gene copy number) and activity were used to calculate the cell-specific activity (Table S4). The cell-specific activity for DNRA ranged from 0.38 to 4.56 fmol N cell⁻¹ d⁻¹, while the cell-specific activity of ammonium oxidizers (AOA & AOB) ranged from 0.32 to 1.75 fmol N cell⁻¹ d⁻¹. Cell-specific activities for both DNRA and NH₄⁺ oxidizers (AOA & AOB) in the fringe riparian zone all exceeded the activities in the central riparian zone, and were highest at A3. This result was consistent with the obtained anammox distribution. Clone analysis further assessed the community composition of DNRA bacteria, symbiotic nitrifiers, and anammox bacteria (Fig. S4). For DNRA bacteria, clone sequences of *nrfA* gene fragments from the fringe riparian zone clustered with *Anaerolinea*, *Anaeromyxobacteraceae*, *Polyangiaceae*, and *Myxococcaceae*. The genera *Anaeromyxobacteraceae*, *Myxococcaceae*, and *Polyangiaceae* all belonging to *Myxobacteria* (Delta-Proteobacteria). Within the order *Myxobacteria*, *Myxococcaceae* and *Polyangiaceae* were identified as aerobic microbes, and only *Anaeromyxobacteraceae* was anaerobic (Sanford et al., 2002). The central riparian zone only had *Anaerolinea*, which is an anaerobic organism that belongs to the phylum *Chloroflexi*. For AOA, the entire archaeal *amoA* gene was most similar to the *Nitrososphaera* cluster, belonging to the group 1.1b lineage, while *Nitrospira* was associated with AOB.

3.5. Ecological significance of anammox and N₂O emission with water level fluctuation

The temporal variability and ecological significance of denitrification and anammox in soils of the riparian zone were investigated in relation to the fluctuation of N₂O emission before and after the change of the groundwater level (range of 50–60 cm depth in 2015 to 20–30 cm depth in 2017). Anammox was also observed to occur after the water level had increased (~30 cm depth), and its distribution trend in each layer was similar to before the increase in water level (Fig. S5). However, the measured potential anammox rate increased significantly compared to before the change of water

level (paired-sample *t*-test, $t = 3.984$, $df = 19$, $p = 0.001$). Based on soil bulk density and microbial activities, the depth-integrated anammox and denitrification rates in the soil core were calculated (Table S7). The anammox and denitrification rates and the contribution of anammox to N loss in the fringe riparian zone all exceeded the activities in the central riparian zone, and were consistently highest at A3.

Before the rise of groundwater level, the depth-integrated anammox rate ranged within 0.29–3.27 mmol-N m⁻² d⁻¹ and contributed 10.2–22.5% to the total N loss (Table S7). This rate was significantly lower than the depth-integrated denitrification rate (2.52–11.22 mmol-N m⁻² d⁻¹; paired-sample *t*-test, $t = 4.169$, $df = 3$, $p = 0.025$; Table S7). The depth-integrated anammox rates however increased to 0.62–8.78 mmol-N m⁻² d⁻¹ after the rise of groundwater level. The contribution ratio of anammox to N loss significantly increased to 22.7–52.3% (paired-sample *t*-test, $t = 5.846$, $df = 3$, $p = 0.010$). The highest depth-integrated anammox rate was observed at A3 in the fringe zone after the water table increased, resulting in the highest contribution of 52.3% to total N-loss.

Furthermore, N₂O fluxes were measured at a high level of 13.2 ± 8.2 mg-N m⁻² h⁻¹ ($n = 24$) in 2015 (before the change of water level), which was significantly higher in the fringe (22.0 \pm 8.2 mg-N m⁻² h⁻¹ at A1, $n = 18$) than in the central riparian zone (7.2 \pm 4.0 mg-N m⁻² h⁻¹ at A12, $n = 6$) (paired-sample *t*-test, $t = 5.666$, $df = 5$, $p = 0.030$; Fig. 6). After the groundwater level increased in 2017, the average N₂O emission gradually decreased with increasing distance from the water in the fringe riparian zone (11.9 \pm 4.2 mg-N m⁻² h⁻¹ at A1, $n = 6$) to the central riparian zone (4.5 \pm 2.5 mg-N m⁻² h⁻¹ at A12, $n = 6$). The average N₂O emission significantly decreased by about 39.3 \pm 10.6% to 7.5 \pm 4.0 mg-N m⁻² h⁻¹ ($n = 24$). Based on these results, the change of the water level influenced the relative contribution of N-loss processes in the riparian zone and shifted denitrification to anammox plus denitrification, with a potential reduction of N₂O emissions.

4. Discussion

This study on riparian zones, which are hotspots for N₂O emissions, provides new information on the role of microbes in N-

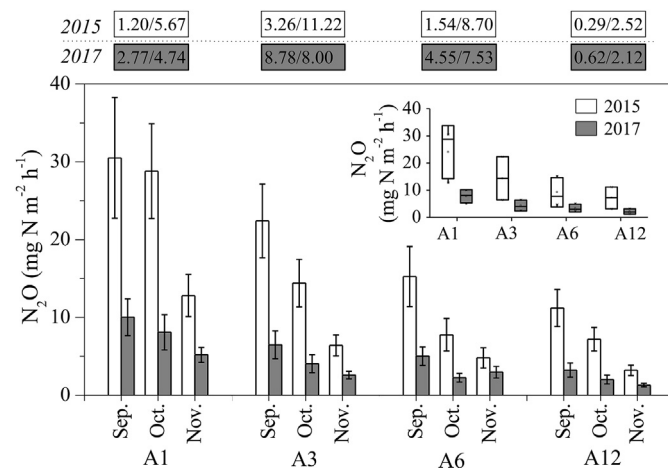


Fig. 6. Temporal N₂O emission flux and depth-integrated rate in the riparian zone with the water level fluctuation in 2015 and 2017. The inset provides statistical results with temporal averaged N₂O emission fluxes (horizontal line indicates the median, box gives the 25th and 75th percentiles, and whisker shows range from the 5th to 95th percentile). The depth-integrated rates were listed in forms of anammox/denitrification on the top. Error bars represent S.D. ($n = 3$).

cycling, wetland management, global change, and N_2O reduction (Hefting et al., 2006; Wang et al., 2006; Groffman et al., 2000; van den Heuvel, 2010). Archaeal and bacterial ammonium oxidation and DNRA with high cell-specific rates drove anammox activity even in oxic subsurface horizons. Furthermore, water tables in riparian ecotones can be managed and optimized to stimulate N-loss and NO_3^- reduction by shifting denitrification to anammox without the threat to increase greenhouse gas emissions. However, several uncertainties remain.

For more than two decades, anammox was generally assumed to only occur in anaerobic environments (Jetten et al., 1998). However, this study showed that anammox actually occurred in all water-saturated soil horizons with high oxygen levels (25–65% oxygen saturation). This high DO could be the result of wetland plants whose reed roots release high levels of oxygen (up to $5.7 \text{ L m}^{-2} \text{ d}^{-1}$, Brix et al., 1996). Approximately 60% of the reed root volume is distributed below a depth of 40 cm (Wang and Yin, 2008), allowing the release of more oxygen into the saturated soil layers. Moreover, since the lake water has a DO above 5 mg L^{-1} , its penetration and fluctuation could have maintained aerobic conditions in the saturated riparian soil ($\text{DO} > 2 \text{ mg L}^{-1}$). However, due to large quantities of organic matter and oxygen-consuming microorganisms in the soil, the soil created an aerobic/anoxic/anaerobic micro-environment, which favors anammox bacteria (Ramakrishnan et al., 2000; Smith et al., 2014). This observation was consistent with the results of anammox zoogloea/granular activated sludge with various particle sizes (1.0–6.4 mm) in different bioreactors, e.g., the completely autotrophic nitrogen removal over nitrite (CANON) process (Third et al., 2001; Vázquez-padrón et al., 2011; Figueroa et al., 2012). Our previous study on municipal wastewater treatment also demonstrated that anammox can occur under aerobic conditions ($\text{DO} > 3 \text{ mg L}^{-1}$) (Wang et al., 2015).

Despite this observation, the activity levels of anammox were lower ($0.01\text{--}0.22 \text{ nmol N g}^{-1} \text{ h}^{-1}$) compared to the activity levels of lake sediments ($0.1\text{--}12.6 \text{ nmol N g}^{-1} \text{ h}^{-1}$, Zhu et al., 2013a, b), river sediments ($0.07\text{--}1.2 \text{ nmol N g}^{-1} \text{ h}^{-1}$, Wang et al., 2012a, b), and paddy field soils ($0.27\text{--}5.25 \text{ nmol N g}^{-1} \text{ h}^{-1}$, Yang et al., 2015; $0.15\text{--}0.77 \text{ nmol N g}^{-1} \text{ h}^{-1}$, Shan et al., 2016). Moreover, anammox activity did not directly correlate with anammox bacterial abundance, resulting in a lower cell-specific rate ($0.005\text{--}0.168 \text{ fmol N cell}^{-1} \text{ d}^{-1}$) compared to previous studies ($5.18 \text{ fmol N cell}^{-1} \text{ d}^{-1}$, Hou et al., 2013; $9.5\text{--}36.2 \text{ fmol N cell}^{-1} \text{ d}^{-1}$, Shen et al., 2014). Anammox rates correlated strongly with the abundances of specific anammox species. For example, both HTS analysis and RDA showed that the anammox rate was positively correlated with the relative abundance of *Kuenenia* and negatively correlated with *Ca. Brocadia* (*B. fulgida* and *B. anammoxidans*). Previous studies reported that *Ca. Kuenenia* adapt better to high DO ($0\text{--}6.4 \text{ mg L}^{-1}$) than *Ca. B. fulgida* ($<0.032 \text{ mg L}^{-1}$) and *Ca. B. anammoxidans* (2.24 mg L^{-1}) (Oshiki et al., 2016). Therefore, the high DO concentration may have inhibited *Ca. Brocadia* activity, but not that of *Ca. Kuenenia*. Despite their presence in low abundances with a finite cell-specific rate, anammox bacteria (*Ca. Kuenenia*) facilitated low anammox activity in aerobic subsurface saturated soil horizons.

Twenty years ago, DNRA was assumed to be negligible in most subsurface environments (Tiedje et al., 1982). In this study, DNRA activity was 10 times higher than the activities of anammox and denitrification with consistent community in subsurface saturated soil horizons; moreover, DNRA was responsible for 88–93% of dissimilatory NO_3^- reduction. Previous studies showed that the DNRA rates in various soils significantly correlate to TN, C/NO_3^- , and C/N ratios (Risgaard-Petersen et al., 2004; Chen et al., 2015; Shan et al., 2016). Usually, DNRA is considered advantageous over denitrification in NO_3^- -limiting conditions, since the high C/N (or NO_3^-) ratios stimulate DNRA bacteria to utilize electron acceptors (i.e.,

NO_3^-) more efficiently when the C source is abundant (Tiedje et al., 1982; Jørgensen et al., 1989; Kraft et al., 2014). In this study, the NO_3^- levels were in the same range of the reported value ($0.8\text{--}2.3 \text{ mg kg}^{-1}$), while the C/N ratios (25–30) were comparatively higher among the different soils (10–18; Shan et al., 2016; Risgaard et al., 1996). This would promote high DNRA partitioning over denitrification in subsurface saturated soil horizons. In addition, analysis of the DNRA *nrfA* gene fragments of the fringe riparian zone indicated that several aerobic microbes potentially performed DNRA, which is consistent with recent research results. During the last years, several studies reported DNRA under different oxygenic conditions including slurry, intact cores, and water columns with more than 80% of oxygen saturation levels (Roberts et al., 2014; Song et al., 2014; Bonaglia et al., 2016). Moreover, the cell-specific activity of aerobic subsurface saturated soil ($0.38\text{--}4.56 \text{ fmol N cell}^{-1} \text{ d}^{-1}$) was also higher than previously reported for anoxic estuarine sediments ($0.22\text{--}0.23 \text{ fmol N cell}^{-1} \text{ d}^{-1}$, Song et al., 2014).

Recently, a number of studies have reported DNRA as an important intermediate process of N cycling in the oceanic ecosystem (Lam et al., 2009; Jensen et al., 2011), the terrestrial aquatic ecosystem (Wang et al., 2018), and soil systems (Shan et al., 2016; Zhu et al., 2018a, b, c). Anammox coupled with DNRA plays a strong role in N loss in marine ecosystems such as in the Arabian Sea (Jensen et al., 2011), the Benguela upwelling system (Kuypers et al., 2005), and the Black Sea (Lam et al., 2009). DNRA provides the necessary NH_4^+ for anammox in these NH_4^+ limiting environments. However, the mechanisms underlying this coupling of anammox–DNRA processes in riparian subsurface saturated soils horizons differ from those in the marine ecosystem since NH_4^+ was not the limiting factor. In the present study, the NO_2^- generation by ammonium oxidation ($3.3\text{--}8.4 \text{ nmol N g}^{-1} \text{ h}^{-1}$) was much higher than the NO_2^- consumption by anammox ($0.03\text{--}0.19 \text{ nmol N g}^{-1} \text{ h}^{-1}$) and denitrification ($0.09\text{--}0.23 \text{ nmol N g}^{-1} \text{ h}^{-1}$) under oxic conditions. Ammonium oxidation produced a NO_2^- surplus for anammox and denitrification, the accumulation of which could exert toxic effects on microbial growth (Bollag et al., 1978). Moreover, a large amount of NH_4^+ was aerobically oxidized, leading to less availability for anammox. In this study, DNRA activity was comparable to that of ammonium oxidation, and reduced the surplus NO_2^- and eliminated toxic inhibition. At the same time, DNRA also provided the necessary NH_4^+ substrate required for anammox. Hence, based on these results, we propose that the coupling of anammox with ammonium oxidation and DNRA promoted the high N-loss observed in subsurface saturated soil horizons.

Measurement of *in-situ* flux further indicated that N_2O flux decreased following an increase in the groundwater level, which is associated with a shift from denitrification to anammox as the dominant N-loss pathway. This verified previous results suggesting that the ecological effect of N_2O mitigation can be attributed to anammox. Our previous studies of the riparian zone in the Three Gorges Reservoir (water level fluctuating 145–175 m above sea level twice per year) showed that N_2O fluxes at the soil–water interface during the flooding period were lower than during the non-flooding period, along with an increase of the abundance of anammox bacteria (Zhu et al., 2015). That study only reported the data on anammox abundance but not on its activity. The present study verified the possible N_2O mitigation effect of anammox by obtaining information on bacterial abundance, activity, and the depth-integrated rate calculation of anammox. Other natural factors such as microbial nitrification, hydrologic conditions, water-quality gradients, and plants (among others) could also affect N_2O emissions when the conditions change from flooding to non-flooding (Hernandez and Mitsch, 2006; Santoro et al., 2011). Previous studies showed that the contribution of nitrifier denitrification to N_2O release gradually decreased with increasing water

levels and DO (Kool et al., 2011; Zhu et al., 2013a, b). This suggests heterotrophic denitrification as the main microbial process producing N_2O in this study. Previous studies, which included both process and mechanistic analyses, have clearly shown that substantial anammox activity could mitigate undesirable N_2O emissions (Kartal et al., 2011; Zhu et al., 2011, 2013a, b). This N_2O mitigation should be attributed to a shift in the dominance of the N-loss pathway from a denitrification to an anammox process, where anammox bacteria directly oxidized NH_4^+ with NO_2^- to N_2 without N_2O emissions. This suggests that the sites that experience substantial N loss via the anammox process will have lower N_2O fluxes than sites that are dominated by denitrification.

In the field of wetland ecology, this result also provides a suggestion for the currently applied management practices, in comparison to historical and less anthropogenically influenced systems. Riparian zones, known as productive N-cycle ecosystems, are important N_2O sources that use denitrification as the main contributor (Hefting et al., 2003; Wang et al., 2012a, b). This study clearly demonstrated that vertically, in the riparian zone, denitrification with potential N_2O emission dominated the cumulative N-losses in the upper unsaturated layers, while anammox activity was higher in lower saturated soil horizons. Moreover, contribution of anammox to N-loss after increasing water level also increased, accompanied by a decrease of N_2O emission. This result provides valuable information for a more effective riparian environmental management. Anthropologically-induced environmental changes (i.e., groundwater table modification) are expected to increase in the future and further change the relative contribution of N-loss from denitrification to the more environmentally friendly anammox pathway. This could significantly impact the cumulative N-budget at a given location, thus bridging global change and local management practices.

5. Conclusions

This study investigated the distribution, biogeochemistry, and microbial mechanisms of denitrification, anammox, damo, and DNRA in different riparian soil horizons, and quantified the contribution of these microbial processes to N-cycle, nitrate-removal, and mitigation of N_2O emission. The following conclusions can be drawn from this study:

- Anammox bacteria were only detected in subsurface saturated soil horizons. Its activity and contribution to N loss increased with depth. In contrast, denitrification was observed in every layer of all sampling sites; however, its abundance and activity decreased with depth. Little to no damo was observed in the same layers. Denitrification dominated the N-losses in the upper unsaturated soil, while, anammox dominated in subsurface saturated soil horizons.
- In riparian subsurface saturated soil horizons, the dominant *Ca. Brocadia* (*Ca. B. fulgida* (62.2%, center) and *Ca. B. anammoxidans* (34.1%, fringe)) also formed an important link between anammox taxa in the riparian center and fringe zone, respectively.
- The key substrate (NO_2^-) for both anammox and denitrification was mainly supplied by NH_4^+ oxidation (54.0–80.4%), and DNRA (51.0–68.4%) consumed a significant proportion of the NH_4^+ required for anammox in riparian subsurface saturated soil horizons.
- After the increase of the groundwater level, the depth-integrated anammox rates increased to $0.62\text{--}8.78\text{ mmol-N m}^{-2}\text{ d}^{-1}$ and the role to N loss significantly increased up to 52.3%. As a result, the average N_2O emission was significantly decreased by $39.3 \pm 10.6\%$, and gradually decreased from the

fringe riparian zone ($11.9 \pm 4.2\text{ mg-N m}^{-2}\text{ h}^{-1}$) to the central riparian zone ($4.5 \pm 2.5\text{ mg-N m}^{-2}\text{ h}^{-1}$).

Declaration of interests

☐ The authors declare that they have no known competing financial interests or personal relationships that could have appeared to influence the work reported in this paper.

Conflicts of interest

We declare no conflict of interest.

Acknowledgements

This research is financially supported by the National Natural Science Foundation of China (No. 41671471, 41322012 and 91851204), Strategic Priority Research Program of the Chinese Academy of Sciences (XDB15020303), National Key R&D Program (2016YFA0602303), Local Innovative and Research Teams Project of Guangdong Pearl River Talents Program (2017BT01Z176), special fund from the State Key Joint Laboratory of Environment Simulation and Pollution Control (Research Center for Eco-environmental Sciences, Chinese Academy of Sciences) (18Z02ESPCR), Open Research Fund of Key Laboratory of Drinking Water Science and Technology, Chinese Academy of Sciences (16Z03KLDWST) and Program of the Youth Innovation Promotion Association (CAS).

Appendix A. Supplementary data

Supplementary data to this article can be found online at <https://doi.org/10.1016/j.watres.2019.06.052>.

References

- Bao, S.D., 2000. Chemical Analysis for Agricultural Soil. China Agriculture Press, Beijing.
- Bollag, J.M., Henninger, N.M., 1978. Effect of nitrite toxicity on soil bacteria under aerobic and anaerobic conditions. *Soil Biol. Biochem.* 10, 377–381.
- Bonaglia, S., Klawonn, I., De Brabandere, L., Deutsch, B., Thamdrup, B., Brüchert, V., 2016. Denitrification and DNRA at the Baltic Sea oxic–anoxic interface: substrate spectrum and kinetics. *Limnol. Oceanogr.* 61, 1900–1915.
- Brix, H., Sorrell, B.K., Schierup, H.H., 1996. Gas fluxes achieved by in situ convective flow in *Phragmites australis*. *Aquat. Bot.* 54, 151–163.
- Burgin, A.J., Hamilton, S.K., 2007. Have we overemphasized the role of denitrification in aquatic ecosystems? A review of nitrate removal pathways. *Front. Ecol. Environ.* 5, 89–96.
- Caporaso, J.G., Kuczynski, J., Stombaugh, J., Bittinger, K., Bushman, F.D., Costello, E.K., Fierer, N., Peña, A.G., Goodrich, J.K., Gordon, J.I., Huttley, G.A., Kelley, S.T., Knights, D., Koenig, J.E., Ley, R.E., Lozupone, C.A., McDonald, D., Muegge, B.D., Pirrung, M., Reeder, J., 2010. QIIME allows analysis of high-throughput community sequencing data. *Nat. Methods* 7 (5), 335–336.
- Chen, Z.M., Ding, W.X., Xu, Y.H., Müller, C., Rütting, T., Yu, H.Y., Fan, J.L., Zhang, J.B., Zhu, T.B., 2015. Importance of heterotrophic nitrification and dissimilatory nitrate reduction to ammonium in a cropland soil: evidences from a ^{15}N tracing study to literature synthesis. *Soil Biol. Biochem.* 91, 65–75.
- Devol, A.H., 2015. Denitrification, anammox, and N_2 production in marine sediments. *Annu. Rev. Mar. Sci.* 7 (1), 403–423.
- Deng, W., Wang, Y., Liu, Z., Cheng, H., Xue, Y., 2014. Heml: a toolkit for illustrating heatmaps. *PLoS One* 9 (11), e111988.
- Deutzmann, J.S., Schink, B., 2011. Anaerobic oxidation of methane in sediments of lake constance, an oligotrophic freshwater lake. *Appl. Environ. Microbiol.* 77 (13), 4429–4436.
- Deutzmann, J.S., Stief, P., Brandes, J., Schink, B., 2014. Anaerobic methane oxidation coupled to denitrification is the dominant methane sink in a deep lake. *Proc. Natl. Acad. Sci. U.S.A.* 111 (51), 18273–18278.
- Di, H.J., Cameron, K.C., Podolyan, A., Robinson, A., 2014. Effect of soil moisture status and a nitrification inhibitor, dicyandiamide, on ammonia oxidizer and denitrifier growth and nitrous oxide emissions in a grassland soil. *Soil Biol. Biochem.* 73, 59–68.
- Ettwig, K.F., Butler, M.K., Le, D.P., Pelletier, E., Manganot, S., Kuypers, M.M., Schreiber, F., Dutilh, B.E., Zedelius, J., de Beer, D., Gloerich, J., Wessels, H.J., van Alen, T., Luesken, F., Wu, M.L., van de Pas-Schoonen, K.T., Op den Camp, H.J.,

- Janssen-Megens, E.M., Francoijs, K.J., Stunnenberg, H., Weissenbach, J., Jetten, M.S., Strous, M., 2010. Nitrite-driven anaerobic methane oxidation by oxygenic bacteria. *Nature* 464 (7288), 543.
- Ettwig, K.F., Van Alen, T., van de Pas-Schoonen, K.T., Jetten, M.S., Strous, M., 2009. Enrichment and molecular detection of denitrifying methanotrophic bacteria of the NC10 phylum. *Appl. Environ. Microbiol.* 75 (11), 3656–3662.
- Figuerola, M., Vázquez-Padín, J.R., Mosquera-Corral, A., Campos, J.L., Méndez, R., 2012. Is the CANON reactor an alternative for nitrogen removal from pre-treated swine slurry? *Biochem. Eng. J.* 65 (15), 23–29.
- Francis, C.A., Roberts, K.J., Beman, J.M., Santoro, A.E., Oakley, B.B., 2005. Ubiquity and diversity of ammonia-oxidizing archaea in water columns and sediments of the ocean. *Proc. Natl. Acad. Sci. U.S.A.* 102, 14683–14688.
- Füssel, J., Lam, P., Lavik, G., Jensen, M.M., Holtappels, M., Günter, M., Kuypers, M.M., 2012. Nitrite oxidation in the Namibian oxygen minimum zone. *ISME J.* 6, 1200–1209.
- Gao, H., Schreiber, F., Collins, G., Jensen, M.M., Kostka, J.E., Lavik, G., de Beer, D., Zhou, H.Y., Kuypers, M.M., 2010. Aerobic denitrification in permeable Wadden Sea sediments. *ISME J.* 4, 417–426.
- Granger, J., Sigman, D.M., 2009. Removal of nitrite with sulfamic acid for nitrate N and O isotope analysis with the denitrifier method. *Rapid Commun. Mass Spectrom.* 23, 3753–3762.
- Groffman, P.M., Bouwman, N.J., Zipperer, W.C., Pouyat, R.V., Band, L.E., Colosimo, M.F., 2002. Soil nitrogen cycle processes in urban riparian zones. *Environ. Sci. Technol.* 36, 4547.
- Groffman, P.M., Gold, A.J., Addy, K., 2000. Nitrous oxide production in riparian zones and its importance to national emission inventories. *Chemosphere Global Change Sci.* 2 (3–4), 291–299.
- Hallin, S., Lindgren, P.E., 1999. PCR Detection of genes encoding nitrite reductase in denitrifying bacteria. *PCR detection of genes encoding nitrite reductase in denitrifying bacteria. Appl. Environ. Microbiol.* 65, 1652–1657.
- Hancock, P.J., Boulton, A.J., Humphreys, W.F., 2005. Aquifers and hyporheic zones: towards an ecological understanding of groundwater. *Hydrogeol. J.* 13, 98–111.
- Haroon, M.F., Hu, S., Shi, Y., Imelfort, M., Keller, J., Hugenholtz, P., Yuan, Z., Tyson, G.W., 2013. Anaerobic oxidation of methane coupled to nitrate reduction in a novel archaeal lineage. *Nature* 500 (7464), 567–570.
- Hefting, M., Clément, J.C., Dowrick, D., Cosandey, A.C., Bernal, S., Cimpian, C., Tatur, A., Burt, T.P., Pinay, G., 2004. Water table elevation controls on soil nitrogen cycling in riparian wetlands along a European climate gradient. *Biogeochemistry* 67, 113–134.
- Hefting, M.M., Bobbink, R., De, C.H., 2003. Nitrous oxide emission and denitrification in chronically nitrate-loaded riparian buffer zones. *J. Environ. Qual.* 32 (4), 1194–1203.
- Hefting, M.M., Bobbink, R., Janssens, M.P., 2006. Spatial variation in denitrification and N₂O emission in relation to nitrate removal efficiency in an-stressed riparian buffer zone. *Ecosystems* 9, 550–563.
- Hernandez, M.E., Mitsch, W.J., 2006. Influence of hydrologic pulses, flooding frequency, and vegetation on nitrous oxide emissions from created riparian marshes. *Wetlands* 26 (3), 862–877.
- van den Heuvel, R.N., 2010. Nitrous Oxide Emission Hotspots and Acidic Soil Denitrification in a Riparian Buffer Zone. Utrecht University.
- Hou, L.J., Zheng, Y.L., Liu, M., Gong, J., Zhang, X.L., Yin, G.Y., You, L., 2013. Anaerobic ammonium oxidation (anammox) bacterial diversity, abundance, and activity in marsh sediments of the Yangtze Estuary. *J. Geophys. Res.* 118 (3), 1237–1246.
- Hu, B.L., Shen, L.D., Lian, X., Zhu, Q., Liu, S., Huang, Q., He, Z.F., Geng, S., Cheng, D.Q., Lou, L.P., Xu, X.Y., Zheng, P., He, Y.F., 2014. Evidence for nitrite-dependent anaerobic methane oxidation as a previously overlooked microbial methane sink in wetlands. *Proc. Natl. Acad. Sci. U.S.A.* 111 (12), 4495–4500.
- Jensen, M.M., Lam, P., Revsbech, N.P., Nagel, B., Gaye, B., Jetten, M.S., Kuypers, M.M., 2011. Intensive nitrogen loss over the omani shelf due to anammox coupled with dissimilatory nitrite reduction to ammonium. *ISME J.* 5 (10), 1660–1670.
- Jetten, M.S.M., Strous, M., van de Pas-Schoonen, K.T., Schalk, J., van Dongen, U.G., van de Graaf, A.A., Logemann, S., Muyzer, G., van Loosdrecht, M.C., Kuenen, J.G., 1998. The anaerobic oxidation of ammonium. *FEMS Microbiol. Rev.* 22 (5), 421–437.
- Jia, Z., Conrad, R., 2009. Bacteria rather than archaea dominate microbial ammonia oxidation in an agricultural soil. *Environ. Microbiol.* 11 (7), 1658–1671.
- Jørgensen, K.S., 1989. Annual pattern of denitrification and nitrate ammonification in estuarine sediment. *Appl. Environ. Microbiol.* 55 (7), 1841–1847.
- Kartal, B., Maalcke, W.J., de Almeida, N.M., Cirpus, I., Gloerich, J., Geerts, W., Op den Camp, H.J., Harhangi, H.R., Janssen-Megens, E.M., Francoijs, K.J., Stunnenberg, H.G., Keltjens, J.T., Jetten, M.S., Strous, M., 2011. Molecular mechanism of anaerobic ammonium oxidation. *Nature* 479, 127–130.
- Kool, D.M., Dolfig, J., Wrage, N., van Groenigen, J.W., 2011. Nitrifier denitrification as a distinct and significant source of nitrous oxide from soil. *Soil Biol. Biochem.* 43 (1), 174–178.
- Kuypers, M.M.M., Lavik, G., Woeckel, D., Schmid, M., Fuchs, B.M., Amann, R., Jørgensen, B.B., Jetten, M.S., 2005. Massive nitrogen loss from the Benguela upwelling system through anaerobic ammonium oxidation. *Proc. Natl. Acad. Sci. U.S.A.* 102, 6478–6483.
- Kraft, B., 2014. Competition in nitrate-reducing microbial communities. *Biotechnol. Bioeng.* 62 (2), 135–144.
- Lam, P., Lavik, G., Jensen, M.M., van de Vossenberg, J., Schmid, M., Woeckel, D., Gutiérrez, D., Amann, R., Jetten, M.S., Kuypers, M.M., 2009. Revising the nitrogen cycle in the Peruvian oxygen minimum zone. *Proc. Natl. Acad. Sci. U.S.A.* 106, 4752–4757.
- Marchant, H.K., Ahmerkamp, S., Lavik, G., Tegetmeyer, H.E., Graf, J., Klatt, J.M., Holtappels, M., Walpersdorf, E., Kuypers, M.M.M., 2017. Denitrifying community in coastal sediments performs aerobic and anaerobic respiration simultaneously. *ISME J.* 11 (8), 1799.
- McClain, M.E., Boyer, E.W., Dent, C.L., Gergel, S.E., Grimm, N.B., Groffman, P.M., Hart, S.C., Harvey, J.W., Johnston, C.A., Mayorga, E., McDowell, W.H., Pinay, G., 2003. Biogeochemical hot spots and hot moments at the interface of terrestrial and aquatic ecosystems. *Ecosystems* 6, 301–312.
- Michotey, V., Mejean, V., Bonin, P., 2000. Comparison of methods for quantification of cytochrome cd1-denitrifying bacteria in marine samples. *Appl. Environ. Microbiol.* 66, 1564–1571.
- Mohan, S.B., Schmid, M., Jetten, M., Cole, J., 2004. Detection and widespread distribution of cytochrome *cd1* denitrifying bacteria in marine samples. *Appl. Environ. Microbiol.* 66, 1564–1571.
- Naeher, S., Huguet, A., Roose-Amsaleg, C.L., Laverman, A.M., Fosse, C., Lehmann, M.F., Derenne, S., Zopf, J., 2015. Molecular and geochemical constraints on anaerobic ammonium oxidation (anammox) in a riparian zone of the seine estuary (France). *Biogeochemistry* 123 (1–2), 237–250.
- Naiman, R.J., Décamps, A.H., 1997. The ecology of interfaces: riparian zones. *Annu. Rev. Ecol. Systemat.* 28 (1), 621–658.
- Nielsen, L.P., 1992. Denitrification in sediments determined from nitrogen isotope pairing. *FEMS Microbiol. Ecol.* 86, 357–362.
- Nie, S.A., Li, H., Yang, X.R., Zhang, Z.J., Weng, B.S., Huang, F.Y., Zhu, G.B., Zhu, Y.G., 2015. Nitrogen loss by anaerobic oxidation of ammonium in rice rhizosphere. *ISME J.* 9, 2059–2067.
- Oshiki, M., Satoh, H., Okabe, S., 2016. Ecology and physiology of anaerobic ammonium oxidizing bacteria. *Environ. Microbiol.* 18 (9), 2784–2796.
- Raghoebarsing, A.A., Pol, A., van de Pas-Schoonen, K.T., Smolders, A.J., Ettwig, K.F., Rijpstra, W.I., Schouten, S., Damsté, J.S., Op den Camp, H.J., Jetten, M.S., Strous, M., 2006. A microbial consortium couples anaerobic methane oxidation to denitrification. *Nature* 440 (7086), 918–921.
- Ramakrishnan, B., Lueders, T., Conrad, R., Friedrich, M., 2000. Effect of soil aggregate size on methanogenesis and archaeal community structure in anoxic rice field soil. *FEMS Microbiol. Ecol.* 32 (3), 261–270.
- Risgaard-Petersen, N., Meyer, R.L., Schmidt, M., Jetten, M.S.M., Enrich-Prast, A., Rysgaard, S., Revsbech, N.R., 2004. Anaerobic ammonia oxidation in an estuarine sediment. *Aquat. Microb. Ecol.* 36, 293–304.
- Rysgaard, S., Risgaard-Petersen, N., Sloth, N.P., 1996. Nitrification, denitrification, and nitrate ammonification in sediments of two coastal lagoons in southern France. *Hydrobiologia* 329 (1–3), 133–141.
- Roberts, K.L., Kessler, A.J., Grace, M.R., Cook, P.L.M., 2014. Increased rates of dissimilatory nitrate reduction to ammonium (DNRA) under oxic conditions in a periodically hypoxic estuary. *Geochim. Cosmochim. Acta* 133 (6), 313–324.
- Sanford, R.A., Cole, J.R., Tiedje, J.M., 2002. Characterization and description of *Anaeromyxobacter dehalogenans* gen. nov. sp. nov. an aryl-halo-respiring facultative anaerobic Myxobacterium. *Appl. Environ. Microbiol.* 68 (2), 893–900.
- Santoro, A.E., Buchwald, C., McIlvin, M.R., Casciotti, K.L., 2011. Isotopic signature of N₂O produced by marine ammonia-oxidizing archaea. *Science* 333 (6047), 1282–1285.
- Schloss, P.D., Westcott, S.L., Ryabin, T., Hall, J.R., Hartmann, M., Hollister, E.B., Lesniewski, R.A., Oakley, B.B., Parks, D.H., Robinson, C.J., Sahl, J.W., Stres, B., Thallinger, G.G., Van Horn, D.J., Weber, C.F., 2009. Introducing mothur: open-source, platform-independent, community-supported software for describing and comparing microbial communities. *Appl. Environ. Microbiol.* 75 (23), 7537–7541.
- Shan, J., Zhao, X., Sheng, R., Xia, Y., Ti, C., Quan, X., Wang, S., Wei, W., Yan, X., 2016. Dissimilatory nitrate reduction processes in typical Chinese paddy soils: rates, relative contributions and influencing factors. *Environ. Sci. Technol.* 50 (18), 9972–9980.
- Shen, L.D., Liu, S., He, Z.F., Lian, X., Huang, Q., He, Y.F., Lou, L.P., Xu, X.Y., Zheng, P., Hu, B.L., 2015. Depth-specific distribution and importance of nitrite-dependent anaerobic ammonium and methane-oxidising bacteria in an urban wetland. *Soil Biol. Biochem.* 83, 43–51.
- Shen, L.D., Liu, S., Huang, Q., Lian, X., He, Z.F., Geng, S., Jin, R.C., He, Y.F., Lou, L.P., Xu, X.Y., Zheng, P., Hu, B.L., 2014. Evidence for the cooccurrence of nitrite-dependent anaerobic ammonium and methane oxidation processes in a flooded paddy field. *Appl. Environ. Microbiol.* 80 (24), 7611–7619.
- Smith, A.P., Marín-Spiotta, E., Graaff, M.A.D., Balser, T.C., 2014. Microbial community structure varies across soil organic matter aggregate pools during tropical land cover change. *Soil Biol. Biochem.* 77 (7), 292–303.
- Smith, R.L., Bohlke, J.K., Song, B., Tobias, C., 2015. Role of anaerobic ammonium oxidation (anammox) in nitrogen removal from a freshwater aquifer. *Environ. Sci. Technol.* 49 (20), 12169–12177.
- Song, B., Lisa, J.A., Tobias, C.R., 2014. Linking DNRA community structure and activity in a shallow lagoonal estuarine system. *Front. Microbiol.* 5, 1–10.
- Tamura, K., Dudley, J., Nei, M., Kumar, S., 2007. MEGA4: molecular evolutionary genetics analysis (MEGA) software version 4.0. *Mol. Biol. Evol.* 24, 1596.
- Third, K.A., Sliekers, A.O., Kuenen, J.G., Jetten, M.S., 2001. The CANON system (completely autotrophic nitrogen-removal over nitrite) under ammonium limitation: interaction and competition between three groups of bacteria. *Syst. Appl. Microbiol.* 24 (4), 588–596.
- Throbäck, I.N., Enwall, K., Åsa, J., Hallin, S., 2004. Reassessing PCR primers targeting *nirS*, *nirK* and *nosZ* genes for community surveys of denitrifying bacteria with

- DGGE. FEMS Microbiol. Ecol. 49, 401–417.
- Tiedje, J.M., Sextstone, A.J., Myrold, D.D., Robinson, J.A., 1982. Denitrification: ecological niches, competition and survival. *Antonie Leeuwenhoek* 48 (6), 569–583.
- Trimmer, M., Risgaard-petersen, N., Nicholls, J.C., Engström, P., 2006. Direct measurement of anaerobic ammonium oxidation (anammox) and denitrification in intact sediment cores. *Mar. Ecol. Prog. Ser.* 326 (4), 37–47.
- Vázquez-padín, J.R., Fernández, I., Morales, N., Campos, J.L., Mosquera-corral, A., Méndez, R., 2011. Autotrophic nitrogen removal at low temperature. *Water Sci. Technol.* 63 (6), 1282–1288.
- Verhoeven, J.T., Arheimer, B., Yin, C., Hefting, M.M., 2006. Regional and global concerns over wetlands and water quality. *Trends Ecol. Evol.* 21 (2), 96–103.
- Wang, C.X., Zhu, G.B., Wang, Y., Wang, S.Y., Yin, C.Q., 2012. Nitrous oxide reductase gene (*nosZ*) and N_2O reduction along the littoral gradient of a eutrophic freshwater lake. *J. Environ. Sci.* 25 (1), 44–52.
- Wang, H., Wang, W., Yin, C., Wang, Y., Lu, J., 2006. Littoral zones as the “hotspots” of nitrous oxide (N_2O) emission in a hyper-eutrophic lake in China. *Atmos. Environ.* 40 (28), 5522–5527.
- Wang, S., Radny, D., Huang, S., Zhuang, L., Zhao, S., Berg, M., Jetten, M.S.M., Zhu, G.B., 2017. Nitrogen loss by anaerobic ammonium oxidation in unconfined aquifer soils. *Sci. Rep.* 7, 40173.
- Wang, S.Y., Peng, Y.Z., Ma, B., Wang, S.Y., Zhu, G.B., 2015. Anaerobic ammonium oxidation in traditional municipal wastewater treatment plants with low-strength ammonium loading: widespread but overlooked. *Water Res.* 84, 66–75.
- Wang, S.Y., Wang, W.D., Liu, L., Zhuang, L.J., Zhao, S.Y., Su, Y., Li, Y.X., Wang, M.Z., Wang, C., Xu, L.Y., Zhu, G.B., 2018. Microbial nitrogen cycle hotspots in the plant-bed/ditch system of a constructed wetland with N_2O mitigation. *Environ. Sci. Technol.* 52 (11), 6226–6236.
- Wang, S.Y., Zhu, G.B., Peng, Y.Z., Jetten, M.S.M., Yin, C.Q., 2012a. Anammox bacterial abundance, activity, and contribution in riparian sediments of the pearl river estuary. *Environ. Sci. Technol.* 46 (16), 8834–8842.
- Wang, S., Wang, Y., Feng, X., Zhai, L., Zhu, G., 2011. Quantitative analyses of ammonia-oxidizing archaea and bacteria in the sediments of four nitrogen-rich wetlands in China. *Appl. Microbiol. Biotechnol.* 90 (2), 779–787.
- Wang, W., Yin, C., 2008. The boundary filtration effect of reed-dominated ecotones under water level fluctuations. *Wetl. Ecol. Manag.* 16, 65–76.
- Wang, W.D., Wang, D.L., Yin, C.Q., 2002. A field study on the hydrochemistry of land/inland water ecotones with reed domination. *Acta Hydrochim. Hydrobiol.* 30, 117–127.
- Wang, Y., Zhu, G.B., Harhangi, H.R., Zhu, B.L., Jetten, M.S.M., Yin, C.Q., Op den Camp, H.J., 2012b. Co-occurrence and distribution of nitrite-dependent anaerobic ammonium and methane-oxidizing bacteria in a paddy soils. *FEMS Microbiol. Lett.* 336, 79–88.
- Welsh, A., Cheesanford, J.C., Connor, L.M., Löffler, F.E., Sanford, R.A., 2014. Refined *nrfA* phylogeny improves PCR-Based *nrfA* gene detection. *Appl. Environ. Microbiol.* 80 (7), 2110–2119.
- Yang, X.R., Li, H., Nie, S.A., Su, J.Q., Weng, B.S., Zhu, G.B., Yao, H.Y., Gilbert, J.A., Zhu, Y.G., 2015. Potential contribution of anammox to nitrogen loss from paddy soils in Southern China. *Appl. Environ. Microbiol.* 81 (3), 938–947.
- Zhao, S.Y., Zhang, L.J., Wang, C., Li, Y.X., Wang, S.Y., Zhu, G.B., 2018. High-throughput analysis of anammox bacteria in wetland and dryland soils along the altitudinal gradient in Qinghai–Tibet Plateau. *Open Microbiol. J.* 7 (2), e00556.
- Zhou, J., Deng, Y., Luo, F., He, Z., Tu, Q., Zhi, X., 2010. Functional molecular ecological networks. *mBio* 1, 1592–1601.
- Zhou, L., Wang, S., Zou, Y., Xia, C., Zhu, G., 2015. Species, abundance and function of ammonia-oxidizing archaea in inland waters across China. *Sci. Rep.* 5, 15969.
- Zhu, G.B., Wang, S.Y., Li, Y.X., Zhuang, L.J., Zhao, S.Y., Wang, C., Kuypers, M.M.M., Jetten, M.S.M., Zhu, Y., 2018a. Microbial pathways for nitrogen loss in an upland soil. *Environ. Microbiol.* 20 (5), 1723–1738.
- Zhu, G.B., Wang, S.Y., Ma, B., Wang, X.X., Zhou, J.M., Liu, R.P., 2018b. Anammox granular sludge in low-ammonium sewage treatment: not bigger size driving better performance. *Water Res.* 142, 147–158.
- Zhu, G.B., Wang, S.Y., Wang, W.D., Wang, Y., Zhou, L.L., Jiang, B., 2013a. Hotspots of anaerobic ammonium oxidation at land-freshwater interfaces. *Nat. Geosci.* 6, 103–107.
- Zhu, G.B., Wang, S.Y., Wang, Y., Wang, C.X., Risgaard–Petersen, N., Jetten, M.S.M., Yin, C., 2011. Anaerobic ammonia oxidation in a fertilized paddy soils. *ISME J.* 5, 1905–1912.
- Zhu, G.B., Wang, S.Y., Zhou, L.L., Wang, Y., Zhao, S.Y., Xia, C., Wang, W., Zhou, R., Wang, C., Jetten, M.S., Hefting, M.M., Yin, C., Qu, J., 2015. Ubiquitous anaerobic ammonium oxidation in inland waters of China: an overlooked nitrous oxide mitigation process. *Sci. Rep.* 5, 17306.
- Zhu, G.B., Wang, M.Z., Li, Y.X., Wang, Y., Fei, H.X., Wang, S.Y., 2018c. Denitrifying anaerobic methane oxidizing in global upland soil: sporadic and non-continuous distribution with low influence. *Soil Biol. Biochem.* 119 (1), 90–100.
- Zhu, X., Burger, M., Doane, T.A., Horwath, W.R., 2013b. Ammonia oxidation pathways and nitrifier denitrification are significant sources of N_2O and no under low oxygen availability. *Proc. Natl. Acad. Sci. U.S.A.* 110 (16), 6328–6333.